Microstructural Model for the Plasticity of Amorphous Solids

M. Hütter,[1] L. C. A. van Breemen[1,2]

[1]*Department of Mechanical Engineering, Polymer Technology, Eindhoven University of Technology, NL-5600 MB Eindhoven, The Netherlands*
[2]*Department of Materials, Polymer Physics, ETH Zürich, CH-8093 Zürich, Switzerland*

Received 30 November 2011; accepted 30 November 2011
DOI 10.1002/app.36576
Published online in Wiley Online Library (wileyonlinelibrary.com).

ABSTRACT: Based on the concept of localized shear transformation zones (STZ), a thermodynamically consistent model for the viscoplastic deformation of amorphous solids is developed. The approach consists of a dynamic description of macroscopic viscoplasticity that is enriched by the evolution of number density and internal structure of the STZ for detailing the origin of viscoplastic flow. So doing, the activation of STZ upon deformation and their subsequent internal re-arrangements are treated as two distinct processes. The detail of the model permits to relate it to small-scale information obtained from experiments or atomistic computer simulations, e.g., in the form of STZ-activation energies and an approximate STZ-volume. The model is illustrated on the example of polycarbonate.
 J Appl Polym Sci 000: 000–000, 2012

Key words: yielding; structure–property relations; amorphous; modeling; microstructure

INTRODUCTION

When solid materials are deformed beyond a critical stress level, processes set in such that any further deformation is not fully recoverable. The origin of such nonelastic behavior is manifold, the most drastic example being failure due to fracture. However, even before that catastrophic mode of failure, a sequence of equally important events occurs, such as initial yielding, followed in many materials by strain-softening, and strain-hardening. In this article, we concentrate on modeling the yielding behavior, particularly of amorphous solids, such as in polymeric and metallic glasses. Specifically, we strive to relate the plastic deformation to the corresponding changes in the microstructure.

The origin of plastic deformation in crystalline solids has been uncovered in terms of crystal defects, namely the dislocations and the associated slip-systems. In metals, the discovery of dislocations goes back to Orowan,[1] Von Polanyi,[2] and Taylor,[3] and had a major impact on the further understanding, modeling, and actual design of metals. While dislocations and slip-systems were discovered and introduced in the field of metals, they also fell on fruitful ground in the field of crystalline polymers, and lead to significant understanding of polymer crystals.[4–8]

Correspondence to: M. Hütter (m.huetter@tue.nl).

A similar story of success for amorphous solids is still to come. Considering the undeformed state, it is a research topic since a considerable time to identify structural differences between the liquid and the glassy state, both being amorphous. Beyond that, the identification of structural changes during mechanical deformation is studied intensely. The experimental work of Argon et al.[9,10] on bubble rafts lead to significant insights. Specifically, the notion of so-called shear transformation zones (STZ) was introduced to denote small regions in which plastic deformation takes place. Such STZ have also been observed experimentally on colloidal systems.[11] Since in many systems the constituent units are too small to be observed, computer simulations have been used instead. For example in amorphous silicon, discrete liquidlike domains have been identified as the carriers of plastic deformation,[12] that come into play upon a critical threshold of stress is reached.[13] Simulations have also been performed on generic model systems, with similar results about localized STZ (see e.g., Refs. [14,15]). Structural signatures have also been elaborated in terms of the inherent structures.[16,17]

Specifically for glassy metals, the microscopic mechanism for steady state inhomogeneous flow in metallic glasses has been studied in the seminal work of Spaepen.[18] It was concluded that the microscopic mechanism for steady state inhomogeneous flow is based on a dynamic equilibrium between stress-driven creation and diffusional annihilation of structural disorder. In agreement, two-dimensional

molecular dynamics simulations of an atomic glass[19] revealed that plastic strain is related to local shear transformations, which were found to be mostly in the same direction as the applied stress. In addition to such simulations (see also Ref. 20), models have been developed for the description of the viscoplastic deformation in metallic glasses.[21]

For the case of amorphous polymeric solids, the structural units for plastic deformation are also intensely debated. For an introduction to the deformation of amorphous polymers, the reader is referred to Ref. 22. An overview of the concepts developed since the middle of the 20th century on concepts concerning the mechanism of plasticity in solid polymers has been compiled by Oleinik.[23] On the basis of published data, it is concluded that the plastic deformation of solid polymers is to some degree accompanied, but not dominated, by chain straightening, at least at small and moderate strains. Rather, short-scale shear transformations are at the kinetic origin of plasticity. The latter conclusion allows factually to draw a close analogy between polymeric and metallic glasses, with respect to yielding. Several models have been developed to describe plastic deformation of solid polymers.[24] While Escaig drew an analogy to crystal plasticity by employing dislocation-like deformation,[25] Robertson[26] presented a molecular model in which the shear-stress is introduced as a bias on the rotational conformation of backbone bonds, producing a polymer structure similar to a liquid above the glass transition. The model predictions were shown to compare favorably with experiments for polystyrene and polymethyl-methacrylate. Later, Argon[27] developed a theory based on thermally activated production of local molecular kinks, and good agreement with experimental data for polystyrene, polyethylene-terephthalate, bisphenol A polycarbonate, and polymethyl-methacrylate was found. Oleinik interpreted experimental data of deformation calorimetric studies, residual strain recovery rate measurements, thermally stimulated creep, DSC, and computer simulation data during plastic deformation in terms of small-scale so-called plastic shear transformations (PST)[28] or anelastic shear transformations (AST).[29] The latter is believed to be a metastable, energetically excited, state of matter that is formed at the early stages of deformation, being the key mechanism for the total kinetics of yielding.[29,30] Also molecular dynamics simulations of glassy polymethylene have shown that inelastic deformation relates to the nucleation of strain-bearing (local) defects rather than to large-scale conformational changes of the polymer coils.[31] Recent direct measurements of molecular mobility before and at yielding of polymer glasses in conjunction with simulations[32,33] support the notion of localized cooperative motions, where the number of those regions increases drastically at the onset of yielding.

From the above, one can draw the conclusion that the origin of plastic deformation in metallic and polymeric systems are related. The question is then how to rationalize such findings in a compact model. What is a first step toward supplementing macroscopic constitutive plastic flow-rules with some details about the actual mechanism of irrecoverable deformation? While some approaches have been mentioned above, the similar observation in different materials calls for a generic modeling approach. In the authors perspective, a significant step in this direction has been undertaken my Falk and Langer.[15] Based on the analysis of molecular dynamics simulations, Langer et al. devised a two-state model[15] capturing the evolution of the density and orientation of the STZ. That description was further developed in Refs. 34 and 35. It is to these works that we will refer to repeatedly when developing our thermodynamically admissible model.

As already stated, there are different terms associated to the localized transformation regions in the process of plastic deformation in amorphous solids, such as STZ, PST, and AST. In the remainder of the article, we shall call them all STZ.

The manuscript is organized as follows. The model for describing the plastic deformation or amorphous solids is introduced in general in the following section. Specifically, the approach entails to combine a macroscopic model for elasto-viscoplastic deformation with the microstructural evolution in terms of STZ. Following these two levels simultaneously, one will learn about the mutual influences between the macroscopic and microstructural levels of description. Then, the material specificity of the model is discussed, as well as the relation to the work of Langer et al.[15,34,35] Finally, the rate-dependent plastic deformation behavior of polycarbonate is studied.

DEVELOPMENT OF THE MODEL

The development of the model is driven by the goal to resolve the dynamics behind the plastic strain rate tensor as it occurs in macroscopic approaches to elasto-viscoplasticity. On the one hand, experimental techniques and computer simulations allow us to gain ever more detailed insight about the processes in the plastic deformation of amorphous solids. On the other hand, it is important to put such insight at work in a concrete model. For that purpose, the STZ-model as elaborated on by Langer et al.[15,34,35] is examined and further developed.

Dynamic variables of interest

It has been shown earlier that for describing the (possibly anisotropic) elasto-viscoplastic behavior of

materials on the macroscopic scale, the elastic part of the deformation gradient is a convenient measure for the state of recoverable deformation, in an Eulerian setting.[36,37] More specifically, it has been shown how a thermodynamically sound class of models can be derived in terms of the quantities of the momentum density per unit volume $\mathbf{u}$, elastic part of the deformation gradient $\mathbf{F}^e$, and a thermal variable, e.g., the internal energy per unit volume e. We point out that, since the plastic deformation is assumed not to change the specific volume, we can use $\det\mathbf{F} = \det\mathbf{F}^e$, and thus the mass density per unit volume is given by means of $\rho = \rho_0 / \det\mathbf{F}^e$. In such a model, the microscopic origins of plastic deformation are encoded rather indirectly in some constitutive law. In view of dealing with potentially anisotropic materials, one may think of choosing the elastic part of the right Cauchy-Green deformation tensor $\mathbf{C}^e = \mathbf{F}^{e,T} \cdot \mathbf{F}^e$ instead of $\mathbf{F}^e$ as a measure of the elastic deformation. However, it must be pointed out that in a Eulerian setting, as we adopt here, the kinematic equation for $\mathbf{C}^e$ is not closed in terms of $\mathbf{C}^e$ itself, but rather involves additionally $\mathbf{F}^e$. Therefore, $\mathbf{C}^e$ is not a suitable replacement for $\mathbf{F}^e$.

To account for the microscopic origin of plastic deformation, one can embed in the macroscopic model of elasto-viscoplasticity a description of the microstructure evolution. Clearly, the success of the approach depends on what quantities are chosen for the quantities of the microstructure as is relevant for the plastic deformation. Our approach taken here rests on the assumption that STZ are the main cause for the plastic deformation. Therefore, a number density of such STZ (per unit mass), Λ, is a reasonable variable to look at, in accord also with earlier approaches.[38] While this resembles the choice of a dislocation density for describing the plasticity in crystalline materials, there is a crucial difference. In crystals, the dislocations (that are line defects in the crystals) promote plastic deformation by their moving through the crystal lattice. In contrast, the STZ are not believed to move significantly. Rather they can be envisioned as regions in space of increased mobility within them. In other words, it is their internal rearrangements that is related to plastic flow. If the STZ do not move but nevertheless they should have an effect in the (directed) plastic flow, it is required that for their description we use a tensor of rank higher than zero, i.e., a vector or a matrix. In analogy to Langer et al.,[15,34,35] we use a two-rank orientation tensor $\mathbf{N}$. Physically, the tensor shall be upper-convected since it will carry the interpretation of $\mathbf{N} = \langle \mathbf{nn} \rangle$ with $\mathbf{n}$ the orientation of the STZ, and $\langle \ldots \rangle$ the average over the zones. Note that orientational information is the minimal step beyond the (isotropic; scalar) STZ-density to allow for the fact that there the plastic strain rate has got directionality in three-dimensional space. It is a matter of practical application of the model to decide which structural features are captured by $\mathbf{N}$, i.e., which kinds of rearrangements in the STZ are of most relevance.

In summary, the full set of dynamic variables is given by

$$\mathbf{x} = (\mathbf{u}, \mathbf{F}^e, e, \Lambda, \mathbf{N}) , \tag{1}$$

which are all functions of the spatial position $\mathbf{r}$ and of time t. Note that the tensor $\mathbf{N}$ is constrained, since due to its interpretation $\mathrm{tr}\mathbf{N} = 1$; this will have ramifications when taking partial derivatives.

Formulation of a closed set of evolution equations

Nonequilibrium thermodynamics acts as a guardrail, helping the modeler to cast the understanding of a complex system with internal variables in a form that complies with certain principles of thermodynamics. There is a wide variety of approaches to nonequilibrium thermodynamics modeling, and the relations between many of them have been established.[39,40] Here, we use a derivative of the general equation for the nonequilibrium reversible–irreversible coupling (GENERIC) framework by Grmela and Öttinger.[41–43] In regard to the topic of this article, this method seems to be the most suitable one, in particular owing to its large flexibility in using structural variables and to its applicability to nonisothermal situations. However, rather than using the framework in its original form with two distinct generators and two operators,[41–43] we use a weak formulation in the form of some specific consequences that follow from the full original form. More specifically, an important ingredient in the GENERIC method is the fact that the total energy and the entropy (the generators of the dynamics) must be considered separately, rather than in the combination of a Helmholtz free energy. Furthermore, ramifications of the conditions in the framework concern very specific statements about how the energy and entropy change as a result of reversible and irreversible dynamics, respectively. Making for two generators two statements each leads to four conditions on the dynamics of the system under consideration, as will be elaborated in the following.

According to the GENERIC framework for (thermally and mechanically) closed nonequilibrium systems,[41–43] the first step is to choose the variables that describe the situation of interest. Similar to the procedure in equilibrium thermodynamics, the choice of variables must be such that they are independent and sufficient to capture the essential physics. Such a set of variables shall here be denoted by $\mathbf{x}$. Once the static properties are specified by an appropriate choice of the generators, $E[\mathbf{x}]$ and $S[\mathbf{x}]$, conditions on

the evolution of these generators amounts to conditions on the evolution of the variables $\mathbf{x}$, by way of the chain rule. We define the following conditions (2) as the "weak formulation" of GENERIC:

The reversible dynamics does not affect the total energy and entropy of the system,

$$\left.\frac{d}{dt}E\right|_{\text{rev}} = 0, \tag{2a}$$

$$\left.\frac{d}{dt}S\right|_{\text{rev}} = 0. \tag{2b}$$

The irreversible dynamics leaves the total energy unaffected, while the entropy change is non-negative,

$$\left.\frac{d}{dt}E\right|_{\text{irr}} = 0, \tag{2c}$$

$$\left.\frac{d}{dt}S\right|_{\text{irr}} \geq 0. \tag{2d}$$

While (2a) and (2c) state that the total energy is conserved for closed systems, the dynamics can still lead to re-distribution of the energy between the different contributions, namely (in this study) between kinetic, elastic, STZ-related, and thermal contributions (see particularly "Application of the Model" below for more details).

It is important to emphasize that both for the reversible and the irreversible dynamics, there are two conditions on the dynamics. Only in the case of isothermal conditions, the respective two criteria can me merged into one for the Helmholtz free energy $F = E - TS$ with T the constant temperature. In the following, we shall use the conditions (2) for analyzing the dynamics of STZ embedded in a elasto-viscoplastic continuum.

It is mentioned in passing that, for the application studied here, the condition (2d) is closely related to the so-called Clausius-Duhem inequality.[44–46] The latter is used frequently in continuum mechanics for expressing the second law of thermodynamics.

Form of the evolution equations

General form

To make effective use of the thermodynamic conditions (2), it is beneficial to use certain general properties of the evolution equations, rather than deriving all parts of all evolution equations. For example, a lot can be drawn from purely kinematic arguments, which are linked to understanding the definitions of the variables $\mathbf{x}$. More specifically, the kinematics specifies the advection terms in the evolution equations. These contributions to the evolution equations can (and should) be worked out. In contrast, constitutive relations for the stress tensor or for irreversible processes shall be left unspecified, as they will be studied in the light of the conditions (2). In the following, we thus first write the general form of the evolution equations of the variables (1), namely,

$$\partial_t \mathbf{u} = -\nabla\cdot(\mathbf{v}\mathbf{u}) + \nabla\cdot\boldsymbol{\sigma}, \tag{3a}$$

$$\partial_t \mathbf{F}^{\text{e}} = -\mathbf{v}\cdot\nabla\mathbf{F}^{\text{e}} + \boldsymbol{\kappa}\cdot\mathbf{F}^{\text{e}} - \boldsymbol{\kappa}^{\text{p}}\cdot\mathbf{F}^{\text{e}}, \tag{3b}$$

$$\partial_t e = -\nabla\cdot(e\mathbf{v}) + \boldsymbol{\kappa}:\boldsymbol{\sigma} - \nabla\cdot\mathbf{q}, \tag{3c}$$

$$\partial_t \Lambda = -\mathbf{v}\cdot\nabla\Lambda + \dot{\Lambda}_{\text{nd}}, \tag{3d}$$

$$\partial_t \mathbf{N} = -\mathbf{v}\cdot\nabla\mathbf{N} + \boldsymbol{\kappa}\cdot\mathbf{N} + \mathbf{N}\cdot\boldsymbol{\kappa}^T - 2(\boldsymbol{\kappa}:\mathbf{N})\mathbf{N} + \dot{\mathbf{N}}_{\text{ra}} + \Psi\dot{\Lambda}_{\text{nd}}, \tag{3e}$$

with velocity and its gradient

$$\mathbf{v} = \mathbf{u}/\rho, \tag{4}$$

$$\boldsymbol{\kappa} = (\nabla\mathbf{v})^T. \tag{5}$$

In the momentum balance (3a), the stress tensor $\boldsymbol{\sigma}$, describing the source of momentum, requires a closure described further below. Similarly, the evolution of the nonkinetic energy density (3c) has the usual form, where $\mathbf{q}$ represents the heat flux. To keep the following treatments concise, we neglect thermal conductivity. However, it is straightforward to include it, when desired. The evolution of the elastic deformation gradient (3b) consists of two terms. On the one hand, the first two terms on the right hand side (r.h.s.) of (3b) are of purely kinematic origin, and correspond to affine (elastic) deformation in an Eulerian setting.[36,44] However, upon the onset of plastic flow, the accumulation of elastic deformation is limited, as expressed by the so-called plastic strain rate tensor $\boldsymbol{\kappa}^p$. Because the density of STZ, Λ, is measured per unit mass, it behaves in a flow field as a scalar (rather than a scalar density). This means that it is only advected with the flow field but does not experience any change due to volume change, as expressed by the first term on the r.h.s. of (3d). The second term on the r.h.s., $\dot{\Lambda}_{\text{nd}}$, represents the effects of nucleation and destruction of STZ. The evolution of the STZ-internal re-arrangements (3e) is based on the following arguments. First, the average structure is advected with the flow field ($-\mathbf{v}.\mathbf{N}$) and distorted affinely by the flow field (terms proportional to $\boldsymbol{\kappa}$). The contribution $-2(\boldsymbol{\kappa}:\mathbf{N})\mathbf{N}$ ensures that the trace of the tensor remains unchanged. In the field of liquid crystal polymers, this contribution relates to the Doi-closure.[47–50] Second, $\dot{\mathbf{N}}_{\text{ra}}$ represents the internal structural re-arrangements (ra) of the zones under the action of the applied stress. And finally, the nucleation and

destruction of zones affects the average orientation as well, by a term proportional to $\dot{\Lambda}_{\rm nd}$.

Constraints on $\boldsymbol{\kappa}^{\rm P}$, $\dot{\mathbf{N}}_{\rm ra}$, and $\boldsymbol{\psi}$

It is commonly assumed that the plastic deformation is isochoric. To see how this condition affects the evolution equation of the elastic deformation gradient $\mathbf{F}^e$, we consider the evolution of its isochoric part,

$$\tilde{\mathbf{F}}^{\rm e} = \mathbf{F}^{\rm e}/\sqrt[3]{\det \mathbf{F}^{\rm e}}, \tag{6}$$

with $\det \tilde{\mathbf{F}}^{\rm e} = 1$. It can be shown by direct calculation that upon plastic deformation

$$\partial_t \tilde{\mathbf{F}}^{\rm e}\Big|_{\rm plast} = -\left(\boldsymbol{\kappa}^{\rm p} - \frac{1}{3}(\mathrm{tr}\boldsymbol{\kappa}^{\rm p})\mathbf{1}\right)\cdot \mathbf{F}^{\rm e}. \tag{7}$$

In other words, the plastic strain rate tensor that changes the tensor $\tilde{\mathbf{F}}^{\rm e}$ only on the submanifold given by $\det \tilde{\mathbf{F}}^{\rm e} = 1$ is of very specific form. Conversely, one concludes that the plastic strain rate tensor in (3b) can be written in the form

$$\boldsymbol{\kappa}^{\rm P} = \hat{\boldsymbol{\kappa}}^{\rm P} - \frac{1}{3}(\mathrm{tr}\hat{\boldsymbol{\kappa}}^{\rm P})\mathbf{1}, \tag{8}$$

with $\hat{\boldsymbol{\kappa}}^{\rm P}$ the unconstrained plastic strain rate tensor.

In a similar way, we can proceed to discuss the proper form of the evolution of $\mathbf{N}$ as to preserve the condition $\mathrm{tr}\mathbf{N} = 1$ by the dynamics. With a symmetric tensor $\mathbf{c}$, we can introduce the traceless quantity $\mathbf{N} = \mathbf{c}/\mathrm{tr}\mathbf{c}$. With the material derivative $D_t = \partial_t + \mathbf{v}\cdot\nabla$, one can show

$$D_t\mathbf{N} = \frac{D_t\mathbf{c}}{\mathrm{tr}\mathbf{c}} - \mathbf{N}\frac{\mathrm{tr}(D_t\mathbf{c})}{\mathrm{tr}\mathbf{c}}. \tag{9}$$

If $\mathbf{c}$ shows upper-convected behavior, $D_t\mathbf{c} = \boldsymbol{\kappa}\cdot\mathbf{c} + \mathbf{c}\cdot\boldsymbol{\kappa}^{\rm T}$, then all $\boldsymbol{\kappa}$-related terms in (3e) including the Doi-closure are recovered by (9). In addition to that, one learns from (9) that $\dot{\mathbf{N}}_{\rm ra}$ and $\boldsymbol{\psi}$ can be written in the form (now assuming $\mathrm{tr}\mathbf{c} = 1$)

$$\dot{\mathbf{N}}_{\rm ra} = \hat{\dot{\mathbf{N}}}_{\rm ra} - (\mathrm{tr}\hat{\dot{\mathbf{N}}}_{\rm ra})\mathbf{N}, \tag{10}$$

$$\boldsymbol{\Psi} = \hat{\boldsymbol{\Psi}} - (\mathrm{tr}\hat{\boldsymbol{\Psi}})\mathbf{N}. \tag{11}$$

Since the internal re-arrangement of zones is at the origin of plastic deformation, one can make the natural choice

$$\xi\hat{\dot{\mathbf{N}}}_{\rm ra} = \hat{\boldsymbol{\kappa}}^{\rm P}, \tag{12}$$

with a scalar prefactor ξ and $\hat{\boldsymbol{\kappa}}^{\rm P}$ the same unconstrained plastic strain rate as in (8). The close relation between $\boldsymbol{\kappa}^{\rm P}$ and $\dot{\mathbf{N}}_{\rm ra}$ is in agreement with a more detailed study of Falk and Langer.[35] However, we clearly recognize that the constraints $\partial_t(\det\tilde{\mathbf{F}}^{\rm e})_{\rm plast} = 0$ and $\partial_t(\mathrm{tr}\mathbf{N})_{\rm plast} = 0$ lead to distinct modifications in (8) and (12).

Summarizing all of the above, the form of the evolution equations becomes

$$\partial_t\mathbf{u} = -\nabla\cdot(\mathbf{v}\mathbf{u}) + \nabla\cdot\boldsymbol{\sigma}, \tag{13a}$$

$$\partial_t\mathbf{F}^{\rm e} = -\mathbf{v}\cdot\nabla\mathbf{F}^{\rm e} + \boldsymbol{\kappa}\cdot\mathbf{F}^{\rm e} - \xi\left(\hat{\dot{\mathbf{N}}}_{\rm ra} - \frac{1}{3}(\mathrm{tr}\hat{\dot{\mathbf{N}}}_{\rm ra})\mathbf{1}\right)\cdot\mathbf{F}^{\rm e}, \tag{13b}$$

$$\partial_t e = -\nabla\cdot(e\mathbf{v}) + \boldsymbol{\kappa}:\boldsymbol{\sigma}, \tag{13c}$$

$$\partial_t\Lambda = -\mathbf{v}\cdot\nabla\Lambda + \dot{\Lambda}_{\rm nd}, \tag{13d}$$

$$\partial_t\mathbf{N} = -\mathbf{v}\cdot\nabla\mathbf{N} + \boldsymbol{\kappa}\cdot\mathbf{N} + \mathbf{N}\cdot\boldsymbol{\kappa}^T - 2(\boldsymbol{\kappa}:\mathbf{N})\mathbf{N} + \left(\hat{\dot{\mathbf{N}}}_{\rm ra} - (\mathrm{tr}\hat{\dot{\mathbf{N}}}_{\rm ra})\mathbf{N}\right) + \left(\hat{\boldsymbol{\Psi}} - (\mathrm{tr}\hat{\boldsymbol{\Psi}})\mathbf{N}\right)\dot{\Lambda}_{\rm nd}, \tag{13e}$$

where we have neglected the heat flux $\mathbf{q}$ for simplicity. In (13), $\mathbf{v} = \mathbf{u}/\rho$ is the velocity field with the mass density $\rho = \rho_0/\det\mathbf{F}^e$, and $\boldsymbol{\kappa} = \partial\mathbf{v}/\partial\mathbf{r}$ denotes the velocity gradient.

It is now the task of the nonequilibrium thermodynamics treatment to make statements about the constitutive relations for the stress tensor $\boldsymbol{\sigma}$, the unconstrained rate of internal re-arrangements $\hat{\dot{\mathbf{N}}}_{\rm ra}$, and the rate $\dot{\Lambda}_{\rm nd}$ of nucleation and destruction.

Generating functionals

To study the conditions that emerge from the application of the constraints (2), we first specify the functionals for the total energy and entropy in terms of the variables (1) as follows,

$$E = \int\left(\frac{\mathbf{u}^2}{2\rho} + e\right)d^3r, \tag{14a}$$

$$S = \int s(\mathbf{F}^{\rm e}, e, \Lambda, \mathbf{N})d^3r, \tag{14b}$$

where we have only written the kinetic energy of the volume element in explicit form. The quantity e accounts for all forms of energy but the kinetic energy. From the form of the energy E, it follows $\delta E/\delta\mathbf{u} = \mathbf{u}/\rho = \mathbf{v}$ for the velocity field. Note that all thermo-mechanical properties of the material are encoded in the function for the entropy density, which shall be kept unspecified for the general treatment. Only when simulating the dynamic response for a specific material further below, we will specify the thermodynamic function in more detail.

Given the forms (14), the functional derivatives become

$$\frac{\delta E}{\delta \mathbf{x}} = \begin{pmatrix} \boldsymbol{v} \\ -\frac{v^2}{2}\rho_{,\mathbf{F}^e} = \frac{v^2}{2}\rho\mathbf{F}^{e,-1,T} \\ 1 \\ 0 \\ 0 \end{pmatrix}, \quad \frac{\delta S}{\delta \mathbf{x}} = \begin{pmatrix} 0 \\ s_{,\mathbf{F}^e} \\ s_{,e} \\ s_{,\Lambda} \\ s_{,\mathbf{N}} \end{pmatrix}. \quad (15)$$

We use the notation $y(\mathbf{x})_{,x_i} \equiv (\partial y/\partial x_i)|_{x_{k\neq i}}$ for partial derivatives, where $x_{k\neq i}$ denotes the remaining variables in (1) to be held constant upon differentiation. Note that $s_{,\mathbf{N}}$ is a constrained derivative due to the condition $\mathrm{tr}\mathbf{N} = 1$. The procedure for accounting for this condition in the derivative can be found in Ref. 51.*

Derivation of the constitutive laws

Before applying the conditions (2), we briefly comment on how to calculate the rate of change of a general functional A of the variables $\mathbf{x}$. Using the chain-rule of variational calculus, one obtains

$$\frac{d}{dt}A[\mathbf{x}] = \int \sum_i \frac{\delta A}{\delta x_i(\mathbf{r})}\partial_t x_i(\mathbf{r}) d^3r, \quad (16)$$

where the summation runs over all variables in the set $\mathbf{x}$. In the above, we have tacitly assumed that the integration domain is not changing in time, which is sufficient for our purposes. Therefore, the conditions (2) can be studied readily by combining the functional derivatives (15) with the evolution equations (13). The reversible and irreversible contributions to dA/dt are obtained by inserting in (16) the reversible and irreversible contributions of $\partial_t x_i$, respectively.

Implementation of the condition $\dot{E}|_{\mathrm{rev}} = 0$

The conservation of the total energy during reversible dynamics can be worked out using the chain rule (16). As a result, one finds that the condition (2a) is automatically satisfied, which is the confirmation of the second term on the r.h.s. of (13c).

Implementation of the condition $\dot{S}|_{\mathrm{rev}} = 0$

It can be shown by direct calculation, that the conservation of the entropy during reversible dynamics leads to a constitutive relation for the stress tensor. In particular, one finds

$$\boldsymbol{\sigma} = \left(e - \frac{s}{s_{,e}}\right)\mathbf{1} - \frac{s_{,\mathbf{F}^e}}{s_{,e}}\cdot\mathbf{F}^{e,T} - 2\frac{s_{,\mathbf{N}}}{s_{,e}}\cdot\mathbf{N}. \quad (17)$$

The details of this expression will be discussed further below.

*In summary, one finds $s_{,\mathbf{N}} = s_{,\mathbf{N}}|_{\mathrm{uc}} - (\mathbf{N}: s_{,\mathbf{N}}|_{\mathrm{uc}})\mathbf{1}$, where the subscript "uc" indicates an unconstrained derivative.

Implementation of the condition $\dot{E}|_{\mathrm{irr}} = 0$

The energy depends only on the variables $\mathbf{u}$, $\mathbf{F}^e$ (through ρ), and e. Of all these, only the elastic deformation gradient has got an irreversible contribution to its dynamics, however, that contribution is of isochoric nature, i.e., $\mathrm{tr}\boldsymbol{\kappa}^p = 0$, according to (8). In turn, this implies that the mass density is, by construction, also not affected by the irreversible deformation, and the total energy thus remains constant. This conclusion can be reached also by performing the calculation of $\dot{E}|_{\mathrm{irr}}$ along the lines of (16).

Implementation of the condition $\dot{S}|_{\mathrm{irr}} \geq 0$

The total entropy must be a nondecreasing function of time. Explicitly calculating $\dot{S}|_{\mathrm{irr}}$ one finds the condition

$$\dot{S}|_{\mathrm{irr}} = \int \left[\left(-\left[s_{,\mathbf{F}^e}\cdot\mathbf{F}^{e,T}\right]^{\mathrm{dev}} + \frac{1}{\xi}s_{,\mathbf{N}}\right) : \xi\hat{\dot{\mathbf{N}}}_{\mathrm{ra}} + \left(s_{,\Lambda} + s_{,\mathbf{N}} : \Psi\right)\dot{\Lambda}_{\mathrm{nd}}\right] d^3r \geq 0, \quad (18)$$

with the notation $\mathbf{A} : \mathbf{B} \equiv A_{ij}B_{ij}$ and $[\mathbf{A}]^{\mathrm{dev}} = \mathbf{A} - (1/3)(\mathrm{tr}\mathbf{A})\mathbf{1}$ for the deviatoric part. In (18), we have made use of the fact that $\mathrm{tr}\boldsymbol{\psi} = 0$, in accord with (11). In this entropy production, one observes two thermodynamic fluxes, $\xi\hat{\dot{\mathbf{N}}}_{\mathrm{ra}}$ and $\dot{\Lambda}_{\mathrm{nd}}$, multiplied by their respective thermodynamic forces. Clearly, in the most general case, there can be cross-effects between these different force-flux pairs.

For the purpose of simplification, we assume that cross-couplings are absent. In this case, the fluxes are only related to their own forces,

$$\xi\hat{\dot{\mathbf{N}}}_{\mathrm{ra}} = \hat{\boldsymbol{\kappa}}^{\mathrm{p}} = {}^{(4)}\mathbf{Q} : \left(-\left[s_{,\mathbf{F}^e}\cdot\mathbf{F}^{e,T}\right]^{\mathrm{dev}} + \frac{1}{\xi}s_{,\mathbf{N}}\right), \quad (19)$$

$$\dot{\Lambda}_{\mathrm{nd}} = Q\left(s_{,\Lambda} + s_{,\mathbf{N}} : \Psi\right), \quad (20)$$

with a fourth-rank tensor ${}^{(4)}\mathbf{Q}$ and a scalar Q as kinetic prefactors. While both of these prefactors may be complicated functions of the variables $\mathbf{x}$ (e.g., by way of a dependence on the stress), their choice must not conflict with the inequality $\dot{S}|_{\mathrm{irr}} \geq 0$. Therefore, one obtains the conditions,

$${}^{(4)}\mathbf{Q} \geq \mathbf{0}, \quad (21a)$$

$$Q \geq 0, \quad (21b)$$

where (21a) is to be interpreted as $\mathbf{A} : {}^{(4)}\mathbf{Q} : \mathbf{A} = \sum_{ijkl} A_{ij}\,{}^{(4)}Q_{ijkl}\,A_{kl} \geq 0$ for all tensors $\mathbf{A}$ of rank two.

The final model

Summarizing the above results, the full set of evolution equations is given by (13) with stress tensor

(17), unconstrained plastic strain rate tensor (19), and nucleation/destruction rate (20), and the conditions (21). While the choice of the internal energy density e as a dynamic variable was convenient for the calculations up to that point, it is more useful for the application of the model to change instead to the absolute temperature T as defined by

$$\frac{1}{T} = s_{,e}\,. \tag{22}$$

Actually performing that change of variables, the full set of evolution equations is given by (13), where the internal energy equation is replaced by the temperature equation and the constitutive relations are related to derivatives of the Helmholtz free energy density, rather than to derivatives of the entropy density. In particular, the constitutive relations can be written in the form

$$\boldsymbol{\sigma} = \rho\left(\hat{f}_{,\mathbf{F}^e}\cdot\mathbf{F}^{e,T} + 2\hat{f}_{,\mathbf{N}}\cdot\mathbf{N}\right), \tag{23}$$

$$\xi\hat{\dot{\mathbf{N}}}_{ra} = \hat{\boldsymbol{\kappa}}^p = -\frac{{}^{(4)}\mathbf{Q}}{T} : \rho\left(-\left[\hat{f}_{,\mathbf{F}^e}\cdot\mathbf{F}^{e,T}\right]^{dev} + \frac{1}{\xi}\hat{f}_{,\mathbf{N}}\right), \tag{24}$$

$$\dot{\Lambda}_{nd} = -\frac{Q}{T}\rho\left(\hat{f}_{,\Lambda} + \hat{f}_{,\mathbf{N}} : \boldsymbol{\Psi}\right), \tag{25}$$

with conditions (21), and where $\hat{f} = f/\rho$ denotes the Helmholtz free energy density per unit mass, and $f = e - Ts$ is the Helmholtz free energy density per unit volume. The stress tensor (23) constitutes the definition of a hyperelastic material[44] and is in agreement with Truesdell and Noll, who obtained this expression by equating the rate of entropy production to zero (see p 296 in Ref. 44).

The evolution of the temperature becomes

$$c_v D_t T = \boldsymbol{\kappa} : \boldsymbol{\sigma}^{(S)} + \rho\left(\left[\hat{e}_{,\mathbf{F}^e}\cdot\mathbf{F}^{e,T}\right]^{dev} - \frac{1}{\xi}\hat{e}_{,\mathbf{N}}\right) : \xi\hat{\dot{\mathbf{N}}}_{ra} - \rho\left(\hat{e}_{,\Lambda} + \hat{\Psi} : \hat{e}_{,\mathbf{N}}\right)\dot{\Lambda}_{nd}\,, \tag{26}$$

with $\hat{e}$ the internal energy per unit mass and $c_v = e_{,T}$ the constant-volume heat capacity per unit volume. The symbol $\boldsymbol{\sigma}^{(S)}$ represents the entropic contribution to the stress tensor, obtained from (23) by replacing $\hat{f}$ by $-T\hat{s}$ with $\hat{s}$ the entropy density per unit mass. It is important to emphasize that for all derivatives in (23–26), the quantities $\hat{f}$, $\hat{e}$, and $\hat{s}$ are considered functions of the variables $\mathbf{F}^e$, T, Λ, and $\mathbf{N}$.

It is pointed out that the above model cannot only be formulated using the weak formulation of GENERIC but also follows from the full structure of the framework. In this respect, the above treatment demonstrates which limited set of thermodynamic restrictions, (2a–2d), are most relevant for this class of models.

APPLICATION OF THE MODEL

To make the above model (13a, 13b, 13d, 13e, 21, 23–26) material specific, we need to specify the quantities $\hat{f}$, ${}^{(4)}\mathbf{Q}$, ξ, Q, and $\boldsymbol{\psi}$. This is done in the following. Afterwards, the relation of our approach to the work of Langer[35] is discussed in detail.

Material specificity

First, the static properties of the material are captured by the Helmholtz free energy density per unit mass, $\hat{f}$. We make the assumption that $\hat{f}$ can be approximated by a sum of two contributions, one due to the macroscopic elastic medium ($\hat{f}_{elast}$) and one due to the STZ ($\hat{f}_{STZ}$),

$$\hat{f} = \hat{f}_{elast} + \hat{f}_{STZ}\,. \tag{27a}$$

In analogy to our earlier efforts,[37] the Helmholtz free energy per unit mass of an elastic medium can be expressed in terms of experimentally measurable quantities. In particular, for given values of the isothermal compressibility $1/K$, the isobaric expansion coefficient α, the constant-pressure heat capacity per unit mass c_p, and the elastic shear modulus G, all at a given reference temperature T_0 and pressure p_0, an approximate form of the Helmholtz free energy density can be found by thermodynamic integration[37]

$$\hat{f}_{elast} = \frac{K}{2}\frac{1}{\rho^*(T)}\left(\frac{\rho^*(T)}{\rho} - 1\right)^2 - \frac{p_0}{\rho} + \frac{1}{2}\frac{G}{\rho^*(T)}\,\mathrm{tr}(\tilde{\mathbf{B}}^e - \mathbf{1}) - c_p\frac{(T-T_0)^2}{2T_0}\,, \tag{27b}$$

with $\rho^*(T) = \rho_0\,[1 - \alpha(T - T_0)]$ and ρ_0 the mass density at the reference point T_0 and p_0. Further, we denote by $\tilde{\mathbf{B}}^e$ the isochoric left Cauchy-Green strain tensor $\tilde{\mathbf{B}}^e = \tilde{\mathbf{F}}^e\cdot\tilde{\mathbf{F}}^{e,T}$, where $\tilde{\mathbf{F}}^e = \mathbf{F}^e/\sqrt[3]{\det\mathbf{F}^e}$ is the isochoric deformation gradient. As for the contribution to the Helmholtz free energy density due the STZ, we write

$$\hat{f}_{STZ} = \Lambda\frac{\varepsilon_1}{2}\left(\mathbf{N} - \frac{1}{3}\mathbf{1}\right) : \left(\mathbf{N} - \frac{1}{3}\mathbf{1}\right) + \Lambda\varepsilon_2 + k_B T\Lambda\ln(\Lambda m_0/e)\,, \tag{27c}$$

which the number density of STZ $\Lambda\rho$ and Euler's constant e. The first term on the r.h.s. of (27c) is analogous to the ansatz in liquid-crystalline polymers, and penalizes the orientation ($\varepsilon_1 > 0$). However, since the scope here is not on liquid-crystalline polymers but on STZ, we refrain from using more elaborate free energy expressions developed in that

field of science. Rather, the first term on the r.h.s. should be understood as a Taylor expansion around the (isotropic) equilibrium state. The second contribution allows to account for the fact that the material needs to be excited (i.e., lifted to a higher energy state) to become a STZ and perform a rearrangement ($\varepsilon_2 > 0$).[28,29] The last term accounts for the configurational entropy of arranging the STZ differently within the volume element. For dimensional reasons, a constant m_0 with the unit of a mass must occur in the logarithm. Doing the explicit calculation for the configurational entropy of noninteracting "particles," i.e., explicit counting of states, one finds that $m_0 = \rho v_0$ with v_0 the smallest unit of volume in the discretized phase space. Please note, that in the general treatment in the preceeding sections there are no restrictions on the form of $\hat{f}$. In particular, we have not used the split (27a). Therefore, this application section here can be adapted to more complicated situations [i.e., without the split (27a)] without the need to redo all the general calculations of the thermodynamics.

Second, the effect of STZ nucleation and destruction on the average orientation must be specified. According to (13e), this is achieved by choosing $\boldsymbol{\psi}$ or $\hat{\Psi}$, respectively. The nucleation or destruction of STZ can lead to a change in the average orientation $\mathbf{N}$. It can be shown by a straightforward calculation, that the change in average orientation assumes the form

$$\dot{\mathbf{N}}\big|_{\mathrm{nd}} = -(\mathbf{N} - \mathbf{N}^*)\,\frac{\dot{\Lambda}_{\mathrm{nd}}}{\Lambda}\,, \tag{28}$$

with $\dot{\Lambda}_{\mathrm{nd}}$ the change in the density of STZ. The quantity $\mathbf{N}^*$ denotes the average orientation of nucleated ($\dot{\Lambda}_{\mathrm{nd}} > 0$) or destroyed ($\dot{\Lambda}_{\mathrm{nd}} < 0$) STZ, respectively. For the time being, we assume that the STZ are nucleated with random orientation, and that they may subsequently be oriented by the applied stress, in agreement with Ref. 35. To keep the current treatment concise, we assume that the corresponding choice $\mathbf{N}^* = (1/3)\mathbf{1}$ also holds for the destruction of STZ. In summary, one obtains a relation between $\dot{\Lambda}_{\mathrm{nd}}$ and the average orientation that is captured in (13e) by the choice

$$\hat{\Psi} = \Psi = -\left(\mathbf{N} - \frac{1}{3}\mathbf{1}\right)\frac{1}{\Lambda}\,, \tag{29}$$

which is of the required form (11).

And third, the kinetics of STZ-internal rearrangements and nucleation/destruction is captured by the kinetic quantities ${}^{(4)}\mathbf{Q}$ and Q. For their specification, we must first discuss the parameter ξ which quantifies how the rate of internal rearrangements in (13e) relates to the plastic strain rate in (13b). Therefore, and also with reference to eqs. (3.11) and (3.12) of Langer,[35] ξ is of the form

$$\xi = \varepsilon_0 \Lambda m_{\mathrm{STZ}}\,, \tag{30}$$

with ε_0 a shear-increment of order unity, and m_{STZ} is the mass of a STZ. The argument to that result goes as follows. If all parts of the material was energetically excited to become STZ, then the plastic strain rate tensor would be equal to the rate of STZ-internal rearrangements ($\dot{\mathbf{N}}_{\mathrm{ra}}$) multiplied by the shear-increment ε_0. If only part of the material is excited, i.e., if the volume fraction $\Lambda m_{\mathrm{STZ}} < 1$, an additional factor Λm_{STZ} is needed because the effective plastic strain rate is proportionally smaller. In other words, if the stress forces the STZ to re-arrange internally (irrespective of the density of STZ), an additional factor of ξ is needed in the relation between the plastic strain rate tensor and the stress tensor. In summary, in view of (24), we write

$$\frac{{}^{(4)}\mathbf{Q}}{T} = \frac{\xi}{2\eta}\,{}^{(4)}\mathbf{1}, \qquad \text{(in accordance with a non-Newtonian flow rule)} \tag{31}$$

$$\frac{Q}{T} = Q'\,, \tag{32}$$

with the viscosity η describing STZ-internal rearrangements,

$$\eta = A_0 \tau_0\, \mathrm{e}^{\Delta H/(k_{\mathrm{B}}T)}\,\frac{\bar{\tau}/\tau_0}{\sinh(\bar{\tau}/\tau_0)}\,, \tag{33a}$$

and the equivalent and characteristic stresses, respectively,

$$\bar{\tau} = \sqrt{\frac{1}{2}(\boldsymbol{\sigma}^d : \boldsymbol{\sigma}^d)} \quad , \quad \tau_0 = \frac{k_{\mathrm{B}}T}{v^*}\,. \tag{33b}$$

In (31), ${}^{(4)}\mathbf{1}$ is the fourth-rank identity tensor with ${}^{(4)}\mathbf{1}$: $\mathbf{A} = \mathbf{A}$: ${}^{(4)}\mathbf{1} = \mathbf{A}$ for all second-rank tensors $\mathbf{A}$. The tensorial structure of ansatz (31) is analogous to what is used in eq. (3.11) in Ref. 35 for the plastic strain rate tensor, the latter being co-linear to the deviatoric part of the stress tensor. For the kinetics of structural re-arrangement in the STZ described by η, we assume that an Eyring-type argument is relevant for that stress-activated process.[52–54] In (33), we use A_0 for the fundamental vibration time, ΔH for the activation enthalpy, and v^* for the activation volume. In contrast, it is assumed that the change in the density of STZ, $\dot{\Lambda}_{\mathrm{nd}}$, is directly proportional to its driving force, i.e., $Q' = \mathrm{const}$.

With the above specifications, all required quantities in the full model (13a, 13b, 13d, 13e, 21, 23–26) can be calculated.

Comparison with Langer (Ref. 35)

In this section, we compare our approach in more detail with the work of Langer,[35] specifically with the eqs. (3.11–13) therein. We start with calculating the plastic strain rate tensor $\boldsymbol{\kappa}^{\mathrm{p}}$ (8) and the rate of internal rearrangements $\dot{\mathbf{N}}_{\mathrm{ra}}$(12), which occur in our evolution eqs. (13b) and (13e), respectively. In view of the general form (24) and the kinetics (31), one obtains for the unconstrained rate of re-arrangement and unconstrained plastic strain rate tensor, respectively,

$$\xi\hat{\dot{\mathbf{N}}}_{\mathrm{ra}} = \hat{\boldsymbol{\kappa}}^{\mathrm{p}} = \frac{\xi}{2\eta}\left(\boldsymbol{\sigma}^{\mathrm{dev}}_{\mathrm{elast}} - \frac{1}{\xi}\rho\hat{f}_{,\mathbf{N}}\right), \tag{34}$$

where $\boldsymbol{\sigma}^{\mathrm{dev}}_{\mathrm{elast}}$ denotes the deviatoric part of the elastic stress tensor contribution, i.e., of the terms in the stress tensor (23) related to $\hat{f}_{\mathrm{elast}}$. In turn, the plastic strain rate tensor and the rate of internal rearrangements become

$$\boldsymbol{\kappa}^{\mathrm{p}} = \frac{\xi}{2\eta}\left(\boldsymbol{\sigma}^{\mathrm{dev}}_{\mathrm{elast}} - \frac{1}{\xi}\rho\left[\hat{f}_{,\mathbf{N}} - \frac{1}{3}\mathrm{tr}(\hat{f}_{,\mathbf{N}})\mathbf{1}\right]\right), \tag{35a}$$

$$\dot{\mathbf{N}}_{\mathrm{ra}} = \frac{1}{2\eta}\left(\boldsymbol{\sigma}^{\mathrm{dev}}_{\mathrm{elast}} - \frac{1}{\xi}\rho\left[\hat{f}_{,\mathbf{N}} - \mathrm{tr}(\hat{f}_{,\mathbf{N}})\mathbf{N}\right]\right). \tag{35b}$$

Despite the similarities between (35) and the eqs. (3.11–12) of Langer,[35] several differences are apparent, even when making the choice (30) for ξ. First, the first term on the r.h.s. of (35a) and (35b) is not the deviatoric part of the total stress tensor, but only of the elastic continuum in which the STZ are embedded. Second, more important is the fact that the remaining terms on the r.h.s. of (35a) and (35b) are different, while they are assumed to be equal in Ref. 35. The fact that they must be different in our view can be traced back to the different conditions imposed on the dynamics, i.e., the determinant-related condition $\partial_t(\det\tilde{\mathbf{F}}^{\mathrm{e}})_{\mathrm{plast}} = 0$ in contrast to the trace-related condition $\partial_t(\mathrm{tr}\mathbf{N})_{\mathrm{plast}} = 0$. The only (mathematical) possibility for having identical driving forces for plastic flow and internal rearrangements is to require that $\mathrm{tr}(\hat{f}_{,\mathbf{N}}) = 0$, which is not even satisfied for the harmonic approximation (27c). In Ref. 35, the second term on the r.h.s. of (35) is said to play the role of a back stress. It must be pointed out, however, that the $\hat{f}_{,\mathbf{N}}$ -related contributions in (35) are of different form than the related contribution to the stress tensor (23).

The relation between the change in the STZ density, $\dot{\Lambda}_{\mathrm{nd}}$, and the average orientation of the STZ in our approach differs slightly from the work of Langer.[35] While in his eq. (3.13) only a part of $\dot{\Lambda}_{\mathrm{nd}}$ (related to the nucleation of zones) affect the average orientation, we here include the full $\dot{\Lambda}_{\mathrm{nd}}$ as affecting the average orientation.

For the remainder of this section, we discuss the evolution equation of the density of STZ. In eq. (3.13) in Ref. 35, the driving force for the process does not depend on the average STZ orientation. In contrast, we get in our treatment

$$\dot{\Lambda}_{\mathrm{nd}} = Q'\rho\left[\frac{\varepsilon_1}{2}\left(\mathbf{N} - \frac{1}{3}\mathbf{1}\right) : \left(\mathbf{N} - \frac{1}{3}\mathbf{1}\right) - \varepsilon_2 - k_{\mathrm{B}}T\ln(\Lambda m_0)\right], \tag{36}$$

based on the general density evolution (25) and the Helmholtz free energy density (27). The last contribution on the r.h.s. depends on the number density of already present STZ. As for the other two contributions, one may tune the significance of orientation (i.e., of STZ-internal structure) by the ratio $\varepsilon_1/\varepsilon_2$. To simplify the comparison with Langer,[35] we assume for the remainder of this section that $\varepsilon_1 = 0$. While it still seems that the driving forces between Langer's and our approach differ, we show now that the two can be matched by the following choice of the kinetic prefactor,

$$Q' = Q''\frac{\exp\left(-\frac{\varepsilon_2}{k_{\mathrm{B}}T}\right) - \Lambda m_0}{-\frac{\varepsilon_2}{k_{\mathrm{B}}T} - \ln(\Lambda m_0)}. \tag{37}$$

Note that $Q' > 0$ is satisfied if $Q'' > 0$. Using this form for the kinetic prefactor in (36), one obtains under neglect of orientational contributions,

$$\dot{\Lambda}_{\mathrm{nd}} = k_{\mathrm{B}}TQ''\rho\left(\exp\left(-\frac{\varepsilon_2}{k_{\mathrm{B}}T}\right) - \Lambda m_0\right), \tag{38}$$

in close correspondence to eqs. (2.1) and (3.13) in Ref. 35.

Finally, we comment on a specific ramification of the nucleation and destruction of zones, eq. 36. For $\varepsilon_1 = 0$, the stationary state of the density of STZ is

$$\Lambda|_{\mathrm{stat}} m_0 = \exp\left(-\frac{\varepsilon_2}{k_{\mathrm{B}}T}\right). \tag{39}$$

This relation is also valid for a varying temperature in the sense of a quasi-stationary density, if the nucleation and destruction of STZ is the fastest process in the system. As a result, the relation for the plastic strain rate tensor, eq. (35a), involves an effective viscosity of the form

$$\eta_{\mathrm{eff}} \equiv \frac{\eta}{\xi} = \frac{(m_0/m_{\mathrm{STZ}})}{\varepsilon_0}\exp\left(\frac{\varepsilon_2 + \Delta H}{k_{\mathrm{B}}T}\right)A_0\tau_0\frac{\bar{\tau}/\tau_0}{\sinh(\bar{\tau}/\tau_0)}. \tag{40}$$

Therefore, the activation energy of the overall viscosity in the quasi-static approximation is composed

TABLE I
Form of the Velocity Gradient κ and the Other Imposed Boundary Conditions, with $\dot{\varepsilon}$ the Applied Deformation Rate

Boundary conditions
$\boldsymbol{\kappa}(t) = \begin{pmatrix} \dot{\varepsilon} & 0 & 0 \\ 0 & \boldsymbol{\kappa}_{22} & 0 \\ 0 & 0 & \boldsymbol{\kappa}_{33} \end{pmatrix}$
$\boldsymbol{\sigma}_{22}(t) = \boldsymbol{\sigma}_{33}(t) = -p^0$

The other elements, $\boldsymbol{\kappa}_{22}$ and $\boldsymbol{\kappa}_{33}$, result dynamically from the corresponding boundary conditions on the stress tensor

of two terms, the activation energy for the generation of STZ (ε_2) and the activation energy for their internal rearrangements (ΔH).

SIMULATIONS FOR POLYCARBONATE

Simulation procedure

The evolution equations (13a,13b,13d,13e,21,23–26) with the above specifications were implemented and solved in the software package Mathematica®. All simulations performed assume homogeneous deformation as well as no heat transfer, i.e., adiabatic boundary condition, with the environment. Because the velocity gradient is spatially constant, which is implied by the homogeneous deformation, it is not required to solve the momentum balance (13a). The simulations performed, are either in uniaxial extension or compression, or a combination of these two loading conditions, e.g., cyclic loading. Only one component of the transposed velocity gradient is imposed, see Table I, the other components represent the free boundaries. To solve such a system of equations, boundary conditions for the free boundaries need to be specified, therefore the stress in these boundaries is equal to the negative environmental pressure, see Table I. The parameters used in the material specific model (previous section) are listed in Table II. While the parameter choices from ρ_0 to ΔH are material specific to polycarbonate and have been used earlier for extensive comparison with experimental data,[55,56] the other parameters in Table II are related to the mesoscopic STZ-model and their values are chosen as to illustrate the model.

Results

The simulation results for uniaxial compression and extension are shown in Figure 1, cyclic loading in Figure 2, and relaxation in Figure 3. All figures are organized such that the subfigures (a) and (b) show the response of the macroscopic quantities, i.e., the stress in deformation direction ($\boldsymbol{\sigma}_{11}$) and temperature (T), whereas the subfigures (c) and (d) depict the response of the variables on the mesoscopic level, i.e., the number of STZ's (Λ) and the average orientation of the STZ in deformation direction (N_{11}). In all simulations performed, the applied strain rate was varied between 10^{-4} s^{-1} and 10^{-2} s^{-1}, and the maximum strain simulated in all simulations is 0.25 for extension and −0.25 for compression.

Figure 1 shows the simulation results for uniaxial extension and compression starting from zero strain. On the macroscopic level, one observes that both the yield stress and the temperature increase with increasing strain rate, in good agreement with experimental observations. Due to the increase of temperature during plastic deformation, "thermal softening" is observed, i.e., the decrease of stress upon further plastic deformation. In Figure 1(b), a different slope is seen in the elastic part ($|\varepsilon| < 0.03$) of the deformation, this is the well known thermoelastic effect described by Thompson.[57] On the mesoscopic level, the orientation increases weakly with increasing strain rate. One should note the effect of compressions for $\varepsilon < 0$ on the orientation of STZ's in deformation direction; the zones will all orient in the (22)- and (33)-directions in an equal fashion, however, both N_{22} and N_{33} are not plotted in the same figure for the sake of clarity. The number of zones at the strain $|\varepsilon| = 0.25$ decreases with increasing strain rate, which is due to the shorter duration of the simulation at the higher rates. In the elastic regime, the number of STZ reaches a plateau value, which is given by (39). On the onset of plastic

TABLE II
Material Properties Specific to Polycarbonate for the Thermodynamic Properties and for the Eyring Viscosity at Room Temperature and Atmospheric Pressure,[55,56] as Used in the Example

Property	Value
ρ_0 (kg/m^3)	1197
T_0 (K)	300
p_0 (MPa)	0.1
c_p(J kg^{-1} K^{-1})	1200
α(K^{-1})	65×10^{-6}
K (MPa)	4350
G (MPa)	833
A_0 (s)	1.33×10^{-28}
v^* (m^3)	5.8×10^{-27}
ΔH (J)	4.82×10^{-19}
Q' (Pa^{-1} s^{-1} kg^{-2})	10^{40}
ε_0 (−)	1.0
ε_1 (J)	$25.0 \times k_B T_0$
ε_2 (J)	$2.0 \times k_B T_0$
v_{STZ} (m^3)	v^*
m_{STZ} (kg)	$\rho_0 v_{STZ}$
m_0 (kg)	m_{STZ}

Symbols are explained in the text.

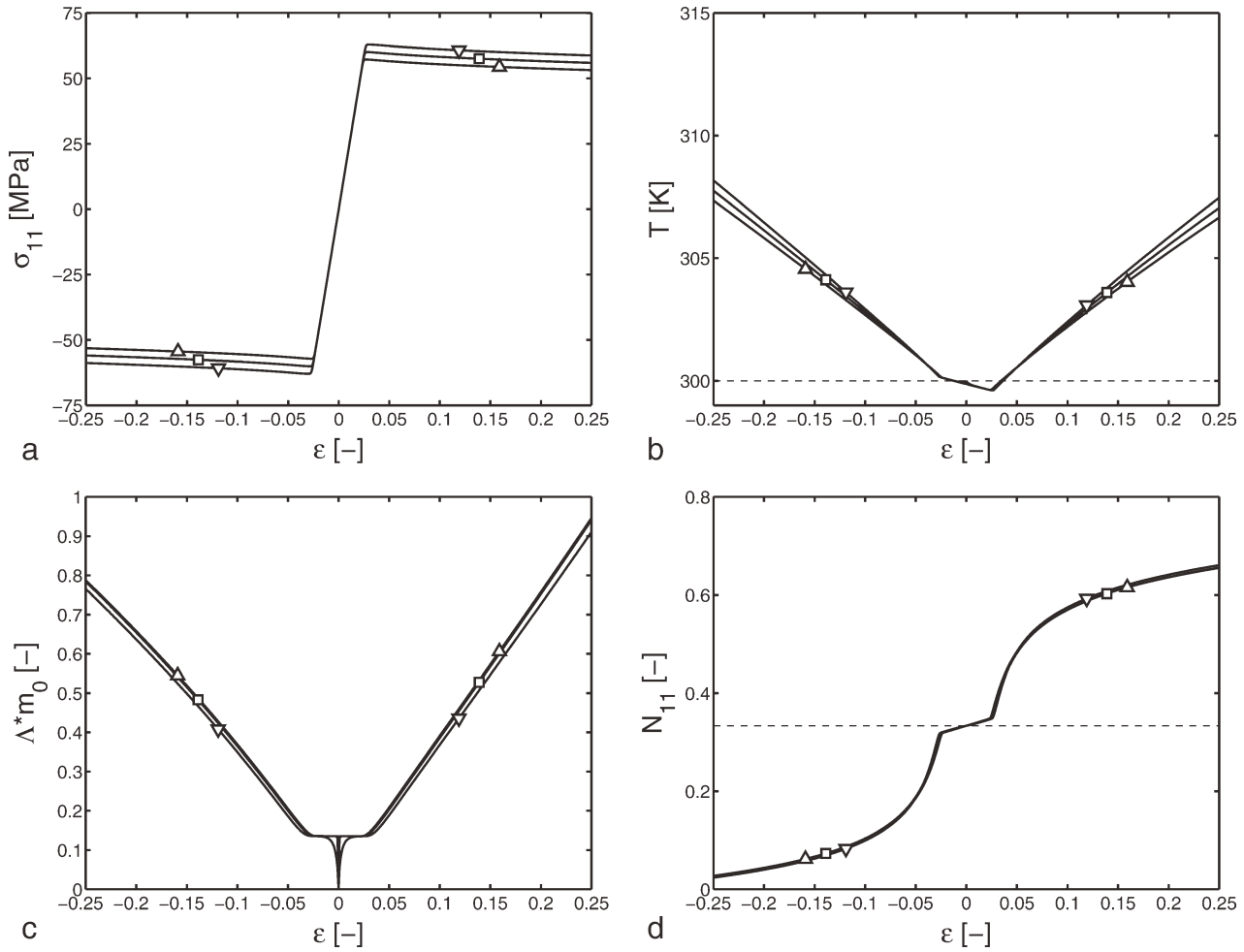

Figure 1 Extension and compression simulations of polycarbonate, with (a) the stress–strain response along the deformation axis, (b) the temperature response, (c) the number of STZ's and (d) the average orientation of STZ's along the deformation axis. The symbols correspond to the applied deformation rates, 10^{-4} s^{-1} (Δ),10^{-3} s^{-1} (□), and 10^{-2} s^{-1} (▽).

deformation, and due to the large value for ε_1, the nucleation of STZ is further promoted [see (36)]. The fact that the transition between the elastic and plastic response is rather sharp is related to the strong stress-dependence of the Eyring viscosity (33). Smoother transitions, in closer correspondence to experiments, can be achieved by adopting a multimode approach.[53]

In Figure 2 for cyclic loading, we observe the expected response of the macroscopic quantities. Particularly, Figure 2(a) shows again the strain-rate influence on yield stress and "thermal softening," and Figure 2(b) exemplifies the viscous heating and the Thompson effect each time when the deformation is elastic. A nice result of the cyclic loading simulations is that one clearly observes that, already after one full cycle, there is an effect on the residual orientation of the STZ's.

The final simulations performed concern relaxation (Fig. 3). After a strain of $\varepsilon_{max} = 0.25$ is reached, the imposed strain rate is set to zero and the evolution of the macroscopic and mesoscopic quantities is monitored. The maximum simulation time corresponds to $t_{sim} = 2\varepsilon_{max}/\dot{\varepsilon}_{max}$ and $t = t_{sim}/2$ corresponds to the instant when the strain rate was set to zero. The stress displays typical viscoelastic response, see Figure 3(a), and decays under constant applied strain. The temperature does not increase when the strain is kept constant. In Figure 3(d), we observe that the zones show only a weak tendency to become more isotropically distributed during stress relaxation; for the conditions considered, the orientation of the zones is rather quenched in a state that does not minimize the Helmholtz free energy density (27c).

Finally, we comment on the simulated values of Λm_0, which for the present set of parameters is equal to the volume fraction of STZ, Λm_{STZ}. The last contribution in the Helmholtz free energy density (27c) is of entropic origin, which reappears in the evolution Eq. (36), last term. This term has the effect that as soon as Λm_0 approaches zero, a very large increase in Λm_0 results; thereby, the entropy effectively ensures that Λm_0 cannot go to (and below)

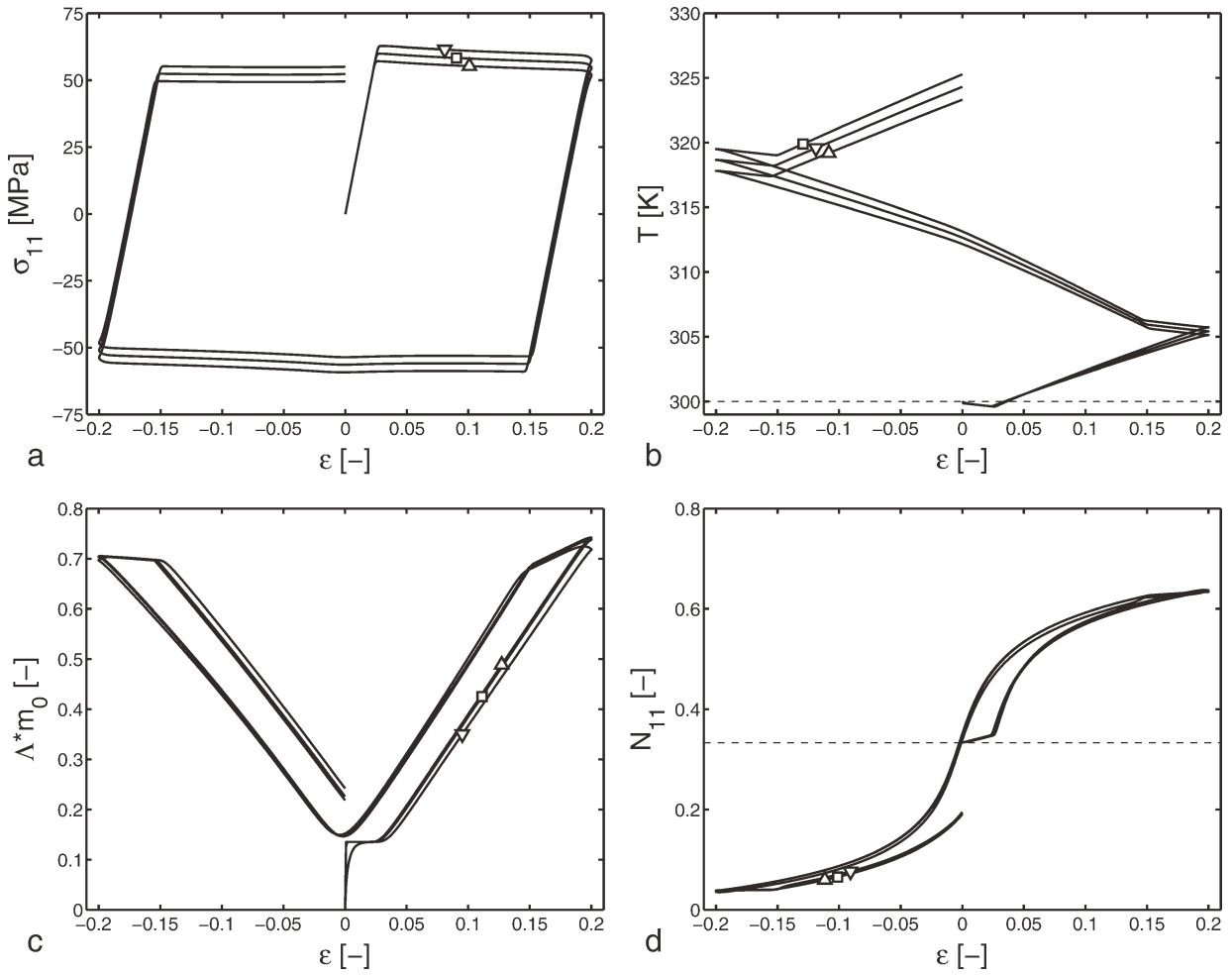

Figure 2 Cyclic loading simulations of polycarbonate, with (a) the stress–strain response along the deformation axis, (b) the temperature response, (c) the number of STZ's, and (d) the average orientation of STZ's along the deformation axis. The symbols correspond to the applied deformation rates, 10^{-4} s^{-1} (Δ),10^{-3} s^{-1} (□), and 10^{-2} s^{-1} (▽).

zero. A similar effect is lacking for the upper limit of close space-filling, $\Lambda m_0 \approx 1$; if included it would affect the behavior in Figures 1(c), 2(c), and 3(c) in the regime of large plastic deformation. Although in principle the corresponding modification of the entropy can be done, it is not straight-forward and hence needs a careful separate discussion. Furthermore, the entropy form chosen in this study leads to a stationary value of the density of STZ that has the Boltzmann form, which is the most common distribution in statistical mechanics, and is readily appreciated. Finally, the comparison with Langer's work is most clear with this specific choice of the entropy, as shown above.

DISCUSSION

Clearly, describing the viscoplastic deformation of glassy solids is a formidable task. It is not even clear if a single model could possibly describe all amorphous materials in a satisfactory manner. However, one can still make an attempt to model a certain class of materials. The approach presented here rests on the following ingredients. First, we have considered solids with a yielding mechanism related to so-called STZ, i.e., localized domains in space with increased mobility. On this basis, there is an interest in the number density of these zones, their size, and their shape (distribution), with the number density being considered most relevant. Here, we have disregarded the shape of the domains, and assumed that they all have approximately the same size. In addition to that, we have chosen an orientational tensor for describing the internal structure of the STZ. As a second main ingredient, we have made use of nonequilibrium thermodynamics (weak formulation of the GENERIC) to link the evolution of STZ-density and internal orientation with the macroscopic deformation of the material. The result is a closed model that explains not only how the macroscopic mechanical deformation affects the mesostructure but also how the mesostructure evolution leads to viscoplasticity. In other words, the mesoscopic and macroscopic levels interact mutually.

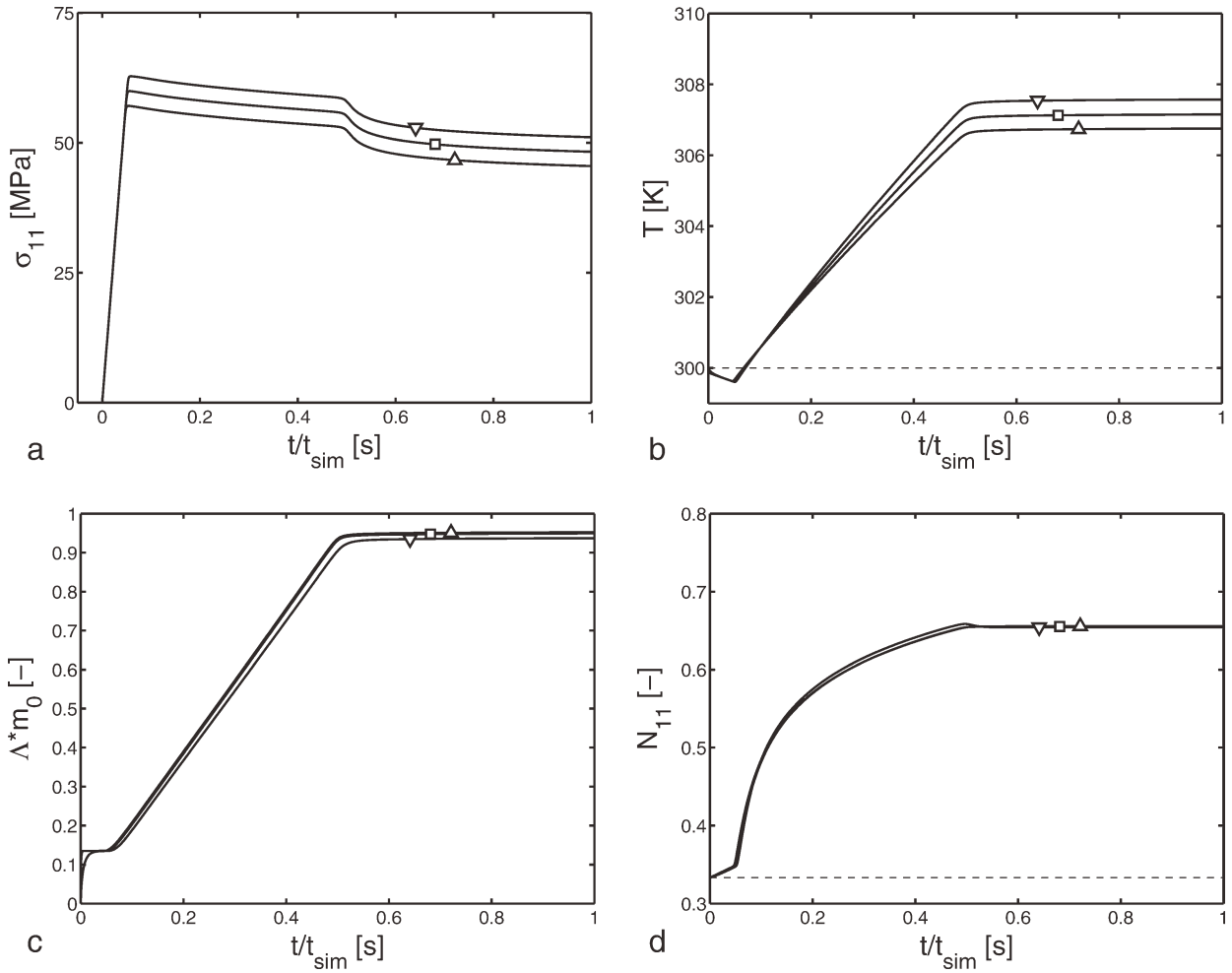

Figure 3 Relaxation simulations of polycarbonate, with (a) the stress–strain response along the deformation axis, (b) the temperature response, (c) the number of STZ's, and (d) the average orientation of STZ's along the deformation axis. The symbols correspond to the applied deformation rates, 10^{-4} s^{-1} (Δ),10^{-3} s^{-1} (□), and 10^{-2} s^{-1} (▽).

The linking of mesoscopic and macroscopic levels in a single approach allows one to make an interesting link between experiments and simulations. Experiments and simulations nowadays give insights about the dynamic heterogeneity before yielding and to regions of nonaffine deformation (see references in the Introduction). Such important information can be accounted for in the model presented in this article. For example, the activation energy for the nucleation of STZ (ε_2) and their internal re-arrangement (ΔH), the size of a STZ (m_{STZ}), and the kinetics and amount of internal rearrangements (η and ε_0) offer concrete possibilities. In turn, the model presented here offers a way to implement chemical specificity not through purely phenomenological parameters, but rather through properties that are more clearly linked to the atomistic detail.

The proposed model is inspired by and compared in detail with the approach of Langer et al.[15,34,35] While the main structure of the mesostructure evolution is the same, differences can be found specifically in the driving forces for STZ-nucleation and for internal re-arrangement. The reason for this discrepancy is obvious. While Langer et al. start from a more microscopic picture with zone populations for given macroscopic stress, we depart from a joint meso-macroscopic approach that also lets the macroscopic continuum evolve. Considering the entire system, more direct use can be made of thermodynamic principles (see section Development of the Model). On the other hand, our approach falls short of considering the configurational/effective temperature being distinct from the absolute temperature. This is important physics for the modeling of glasses, and therefore our current approach clearly needs to be amended in this direction.

For illustration purposes, the behavior of the model is demonstrated for extension and compression, cyclic loading, and for stress-relaxation (see section Simulations for Polycarbonate). While the macroscopic parameters are chosen to represent poly-carbonate, the parameters related to the STZ were chosen by plausibility, due to a lack of clear experimental data. However, once such experimental

data becomes available, our model offers a procedure to incorporate it such that the insights on the mesoscopic scales are coupled to the macroscopic thermo-mechanical behavior in a thermodynamically consistent way.

Finally, we comment on a technical shortcoming of the model presented here. Currently, we have used a rather high value for the orientational effect of the STZ, ε_1, which is in particular significantly higher than the activation energy for STZ nucleation, $\varepsilon_1 \gg \varepsilon_2$. Physically, it may be difficult to argue in favor of such a large value. Technically, this large value was adopted as to prevent some elements of $\mathbf{N}$ becoming unphysical under strong deformation, e.g., $N_{11} < 0$. This shortcoming has a physical origin. The entropy (i.e., the logarithm of the number of available microstates for given $\mathbf{N}$) is minimal if all zones are oriented parallel to each other. The approach to that minimal value is certainly not captured well by the Helmholtz free energy density (27c). In future work we will, with reference to modeling efforts in the field of liquid-crystalline polymers, alleviate this problem by including an entropy expression which approximates the behavior close to perfect orientation adequately.

The authors acknowledge stimulating discussions from Prof. E. F. Oleinik about the various aspects of yielding in amorphous materials.

References

1. Orowan, E. Z Phys 1934, 89, 605.
2. Von Polanyi, M. Z Phys 1934, 89, 660.
3. Taylor, G. I. Proc R Soc London Sec A 1934, 145, 362.
4. Gleiter, H.; Argon, A. S. Philos Mag 1971, 24, 71.
5. Bartczak, Z.; Cohen, R. E.; Argon, A. S. Macromolecules 1992, 25, 4692.
6. Bartczak, Z.; Argon, A. S.; Cohen, R. E. Macromolecules 1992, 25, 5036.
7. Galeski, A.; Bartczak, Z.; Argon, A. S.; Cohen, R. E. Macromolecules 1992, 25, 5705.
8. Lin, L.; Argon, A. S. J Mater Sci 1994, 29, 294.
9. Argon, A. S.; Kuo, H. Y. Mater Sci Eng 1979, 39, 101.
10. Argon, A. S.; Shi, L.-T. Philos Mag A 1982, 46, 275.
11. Schall, P.; Weitz, D. A.; Spaepen, F. Science 2007, 318, 1895.
12. Demkowicz, M.; Argon, A. S. Phys Rev B 2005, 72, 245205.
13. Argon, A. S.; Demkowicz, M. Philos Mag 2006, 86, 4153.
14. Maloney, C. E.; Lemaitre, A. Phys Rev E 2006, 74, 016118.
15. Falk, M. L.; Langer, J. S. Phys Rev E 1998, 57, 7192.
16. Del Gado, E.; Ilg, P.; Kröger, M.; Öttinger, H. C. Phys Rev Lett 2008, 101, 095501.
17. Mosayebi, M.; Del Gado, E.; Ilg, P.; Öttinger, H. C. Phys Rev Lett 2010, 104, 205704.
18. Spaepen, F. Acta Metal 1977, 25, 407.
19. Deng, D.; Argon, A. S.; Yip, S. Philos Trans R Soc Lond A 1989, 329, 613.
20. Albano, F.; Lacevic, N.; Falk, M. L.; Glotzer, S. C. Mater Sci Eng A Struct 2004, 375, 671.
21. Argon, A. S.; Shi, L. T. Acta Metal 1983, 31, 499.
22. Perez, J. Physics and Mechanics of Amorphous Polymers; Balkema: Rotterdam, 1998.
23. Oleinik, E. F.; Rudnev, S. N.; Salamatina, O. B. Polym Sci Ser A 2007, 49, 1302.
24. Crist, B. The Physics of Glassy Polymers, Chapter 4: Yield processes in glassy polymers; Chapman and Hall: London, 1997, p 155–212.
25. Escaig, B. Polym Eng Sci 1984, 24, 737.
26. Robertson, R. E. J Chem Phys 1966, 44, 3950.
27. Argon, A. S. Philos Mag 1973, 28, 839.
28. Oleinik, E. F.; Salamatina, O. B.; Rudnev, S. N.; Shenogin, S. V. Vysokomol Soedin Ser A and Ser B 1993, 35, 1819.
29. Oleinik, E. F.; Rudnev, S. N.; Salamatina, O. B.; Shenogin, S. V.; Kotelyanskii, M. I.; Paramzina, T. V.; Nazarenko, S. I. E-Polymers 2006, 29, 1.
30. Shenogin, S. V.; Hohne, G. W. H.; Salamatina, O. B.; Rudnev, S. N.; Oleinik, E. F. Polym Sci Ser A 2004, 46, 21.
31. Balabaev, N. K.; Mazo, M. A.; Lyulin, A. V.; Oleinik, E. F. Polym Sci Ser A 2010, 52, 633.
32. Lee, H. N.; Paeng, K.; Swallen, S. F.; Ediger, M. D. Science 2009, 323, 231.
33. Riggleman, R. A.; Lee, H. N.; Ediger, M. D.; de Pablo, J. J. Soft Mater 2010, 6, 287.
34. Langer, J. S. Script Mater 2006, 54, 375.
35. Langer, J. S. Phys Rev E 2008, 77, 021502.
36. Hütter, M.; Tervoort, T. A. J Non-Newtonian Fluid Mech 2008, 152, 45.
37. Hütter, M.; Tervoort, T. A. J Non-Newtonian Fluid Mech 2008, 152, 53.
38. Hasan, O. A.; Boyce, M. C.; Li, X. S.; Berko, S. J Polym Sci B Polym Phys 1993, 31, 185.
39. Grmela, M. J Non-Newtonian Fluid Mech 1997, 69, 105.
40. Jongschaap, R. J. J.; Öttinger, H. C. J Non-Newtonian Fluid Mech 2001, 96, 1.
41. Grmela, M.; Öttinger, H. C. Phys Rev E 1997, 56, 6620.
42. Öttinger, H. C.; Grmela, M. Phys Rev E 1997, 56, 6633.
43. Öttinger, H. C. Beyond Equilibrium Thermodynamics; Wiley: Hobroken, 2005.
44. Truesdell, C.; Noll, W. The Non-Linear Field Theories of Mechanics; Springer: Berlin, 1992.
45. Besseling, J. F.; Van der Giessen, E. Mathematical Modelling of Inelastic Deformation, Vol. 5 of Applied Mathematics and Mathematical Computation; Chapman and Hall: London, 1994.
46. Šilhavý, M. The Mechanics and Thermodynamics of Continuous Media; Springer: Berlin, 1997.
47. Larson, R. G. The Structure and Rheology of Complex Fluids; Oxford University Press: New York, 1999.
48. Hinch, E. J.; Leal, L. G. J Fluid Mech 1976, 76, 187.
49. Kröger, M. Models for Polymeric and Anisotropic Liquids, Vol. 675 of Lecture Notes in Physics; Springer: Berlin, 2005.
50. Kröger, M.; Ammar, A.; Chinesta, F. J Non-Newtonian Fluid Mech 2008, 149, 40.
51. Beris, A. N.; Edwards, B. J., Thermodynamics of Flowing Systems with Internal Microstructure; Oxford University Press: Oxford, 1994.
52. Tervoort, T. A.; Smit, R. J. M.; Brekelmans, W. A. M.; Govaert, L. E. Mech Time-Dependent Mater 1998, 1, 269.
53. Tervoort, T. A.; Klompen, E. T. J.; Govaert, L. E. J Rheol 1996, 40, 779.
54. Tervoort, T. A.; Govaert, L. E. J Rheol 2000, 44, 1263.
55. Govaert, L. E.; Timmermans, P. H. M.; Brekelmans, W. A. M. J Eng Mater T ASME 2000, 122, 177.
56. Klompen, E. T. J.; Engels, T. A. P.; Govaert, L. E.; Meijer, H. E. H. Macromolecules 2005, 38, 6997.
57. Thompson, W. Trans R Soc Ed 1853, 20, 261.